EFFECTIVE THERMAL EXPANSION COEFFICIENTS OF COMPOSITES REINFORCED BY TWO-DIMENSIONALLY MISORIENTED SHORT-GLASS-FIBERS

Takao, Yoshihiro
Research Institute for Applied Mechanics Kyushu University : Associate Professor

https://doi.org/10.5109/6781002

出版情報：Reports of Research Institute for Applied Mechanics. 31 (97), pp.15-27, 1983-09. 九州大学応用力学研究所
バージョン：
権利関係：

Reports of Research Institute for Applied Mechanics
Vol. XXXI, No. 97, 1983

EFFECTIVE THERMAL EXPANSION COEFFICIENTS OF COMPOSITES REINFORCED BY TWO-DIMENSIONALLY MISORIENTED SHORT-GLASS-FIBERS

BY Yoshihiro TAKAO*

This paper examines the thermal expansion coefficients of composites containing two-dimensionally misoriented isotropic short fibers. The analysis is based upon the Eshelby's equivalent inclusion method and average induced strain approach, which can take into account the interaction among all fibers at different orientations. Non-dimensional thermal expansion coefficients of Glass/Epoxy composite system are obtained as the function of fiber orientation distribution limit β. The effects of material constants on thermal expansion coefficients are also presented.

Keywords :Thermal expansion, Thermal strain, Misoriented fiber, Random distribution, Glass, Fiber aspect ratio

1. Introduction

Discontinuous-fiber reinforced composites are attractive in their versatility in properties and relatively low-fabrication cost. They consist of relatively short, variable length, and imperfectly aligned fibers distributed in matrix. The orientation of short-fibers depends on the processing conditions employed and may vary from random to nearly aligned[1]. Thus it is imperative to take into account the effects of the bias in fiber orientation and variation in fiber aspect ratio on composite thermoelastic properties. The effective Young's modulus of misoriented short-fiber composites was well studied in recent literatures[2),3)]. Thus we will study the thermal expansion coefficients α_c of composites reinforced by misoriented isotropic short-fibers.

These effects have not been discussed except for the completely random distribution[4)~6)]. Chou and Nomura[4)] and Craft and Christensen[5)] used the so-called classical lamination analogy, where the interaction between all fibers at different orientation is not considered. The work by Takahashi et al[6)]. was based on the Eshelby's equivalent inclusion method[7)~9)], which can take into account the interaction between all fibers and will be used in this paper.

* Associate Professor
Research Institute for Applied Mechanics
Kyushu University

The general approach was already presented[10] for the case of the hybrid composites reinforced by anisotropic fibers such as Carbon or Kevlar. Though theoretically this paper treats the special case of Reference 10, the numerical results itself are new and practically useful for the Glass-fiber composite community. Non-dimensional results of α_c & $(\alpha_c-\alpha_m)/(\alpha_f-\alpha_m)$, in the case of Glass/Epoxy composites are computed for two-dimensinal distribution of fiber orientation with the parameter of distribution limit β. The effects of fiber distribution patterns (uniform or cosine-type), aspect ratio, volume fraction, and material constants are presented.

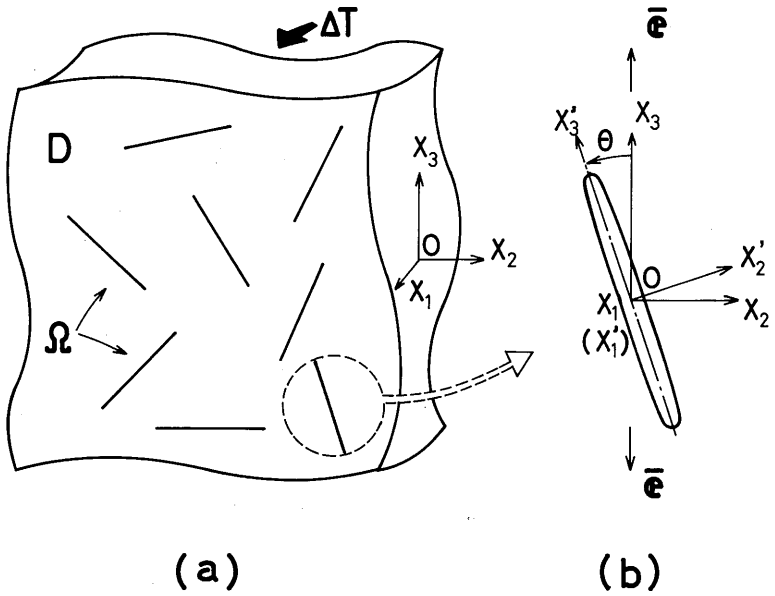

Fig. 1 A calculation model.

2. Basic Equation

Our analytical model consists of misoriented short-fibers which are isotropic and embedded in an infinite isotropic matrix as shown in Fig. 1-a. All fibers are modeled as prolate spheroids. Let the domain of the infinite body and fibers be denoted by D and Ω, respectively. Hence the domain of the matrix becomes $D-\Omega$. Note that Ω can represent a particular inhomogeneity(fiber) or all inhomogeneities. The elastic constants of the matrix and fiber are denoted by $\boldsymbol{C}_m$ and $\mathbf{C}_f$, respectively, and thermal expansion coefficients of matrix and fiber are denoted by $\boldsymbol{\alpha}_m$ and $\boldsymbol{\alpha}_f$, respectively. The bold face letter stands for tensorial quantity. The internal stress $\boldsymbol{\sigma}$ will be induced in the composite due to the

mismatch between $\boldsymbol{\alpha}_m$ and $\boldsymbol{\alpha}_f$ under the temperature change ΔT, and is a function of a position. The volume average of $\boldsymbol{\sigma}$ in $D-\Omega$ defines the volume averaged disturbance of strain in $D-\Omega$, $\bar{\boldsymbol{e}}$, due to the presence of all fibers as follows,

$$\langle\boldsymbol{\sigma}\rangle \ (\equiv \frac{1}{V_{D-\Omega}}\int_{D-\Omega}\boldsymbol{\sigma}dV) = \boldsymbol{C}_m\bar{\boldsymbol{e}} \tag{1}$$

where $\langle\ \rangle$ denotes the volume average of a quantity in $D-\Omega$ and $V_{D-\Omega}$ is the volume of matrix. Now a single fiber is introduced into the field where $\bar{\boldsymbol{e}}$ was applied. The orientation of fiber is defined by angle θ as shown in Fig. 1-b. To apply the Eshelby's equivalent inclusion method to this single fiber the local coordinate system $x_1'x_2'x_3'$ is also adopted, where the x_3' axis coinsides with the fiber axis. In $D-\Omega$ and Ω, the thermal expansion $\boldsymbol{\alpha}_m\Delta T$ and $\boldsymbol{\alpha}_f\Delta T$ are applied, respectively. Without losing generality we take $\Delta T = 1$. Then

$$\boldsymbol{\alpha}^* = \boldsymbol{\alpha}_f - \boldsymbol{\alpha}_m \tag{2}$$

in Ω is related to $\boldsymbol{\sigma}$ in D and the Eshelby's equivalent inclusion method[7)~9)] yields

$$\boldsymbol{\sigma}' = \boldsymbol{C}_m'(\bar{\boldsymbol{e}}'+\boldsymbol{e}'-\alpha^{*'}-\boldsymbol{e}^{*'}) \tag{3-a}$$

in Ω

$$= \boldsymbol{C}_f'(\bar{\boldsymbol{e}}'+\boldsymbol{e}'-\alpha^{*'}) \tag{3-b}$$

and

$$\boldsymbol{e}' = \boldsymbol{S}'(\alpha^{*'}+\boldsymbol{e}^{*'}) \tag{4}$$

where $\boldsymbol{\sigma}'$ is the disturbance of stress due to this single fiber, $\boldsymbol{S}'$ is the Eshelby's tensor[9)], and $\boldsymbol{e}^{*'}$ is the fictitious strain called "eigen strain" or "transformation strain" and has some value in Ω but vanishes in $D-\Omega$. Here the prime indicates tensorial quantity refered to the local coordinate system. Since the added single fiber can be regarded as any fiber in the composite eq. 3 can hold for any inclusion in D. The fact that the volume average of $\boldsymbol{\sigma}$ in D vanishes[9)] leads to

$$\bar{\boldsymbol{e}}+\frac{1}{V_D}\int_{\Omega}T_C(\boldsymbol{S}'-\boldsymbol{I}')(\boldsymbol{\alpha}^{*'}+\boldsymbol{e}^{*'})dV = 0 \tag{5}$$

where V_D, $\boldsymbol{I}$, and T_C denote the volume of D, identity tensor, and transformation from the local to global coordinate system $x_1x_2x_3$, respectively. Here we use that $T_C\boldsymbol{C}_m'T_C^{-1} = \boldsymbol{C}_m$ and $\boldsymbol{C}_m$ is constant in D. T_C^{-1} denotes the transformation from the global to local coordinate system. From eqs. 3 and 4 we obtain

$$\boldsymbol{\alpha}^{*'}+\boldsymbol{e}^{*'} = \{(\boldsymbol{C}_f'-\boldsymbol{C}_m')(\boldsymbol{S}'-\boldsymbol{I}')+\boldsymbol{C}_f'\}^{-1}\times \{\boldsymbol{C}_f'\boldsymbol{\alpha}^{*'}-(\boldsymbol{C}_f'-\boldsymbol{C}_m')T_C^{-1}\bar{\boldsymbol{e}}\} \tag{6}$$

A substitution of eq. 6 into eq. 5 yields

$$(\boldsymbol{I}-\frac{1}{V_D}\int_\Omega T_C\boldsymbol{G}_1'T_C^{-1}dV)\bar{\boldsymbol{e}} = -\frac{1}{V_D}\int_\Omega T_C\boldsymbol{G}_2'\boldsymbol{\alpha}^{*'}dV \tag{7}$$

where

$$\begin{aligned}\boldsymbol{G}_1' &= (\boldsymbol{S}'-\boldsymbol{I}')\{(\boldsymbol{C}_f'-\boldsymbol{C}_m')(\boldsymbol{S}'-\boldsymbol{I}')+\boldsymbol{C}_f'\}^{-1}(\boldsymbol{C}_f'-\boldsymbol{C}_m')\\ \boldsymbol{G}_2' &= (\boldsymbol{S}'-\boldsymbol{I}')\{(\boldsymbol{C}_f'-\boldsymbol{C}_m')(\boldsymbol{S}'-\boldsymbol{I}')+\boldsymbol{C}_f'\}^{-1}\boldsymbol{C}_f'\end{aligned} \tag{8}$$

The volume average of the induced strain in D due to $\boldsymbol{\alpha}^*$ and $\boldsymbol{e}^*$, $\boldsymbol{\gamma}_D$, is obtained as follows[9],

$$\boldsymbol{\gamma}_D = \frac{1}{V_D}\int_\Omega \boldsymbol{\alpha}^*+\boldsymbol{e}^*dV \tag{9}$$

Substituting eq. 6 into eq. 9 after the transformation to the global coordinate system, we finally obtain $\boldsymbol{\alpha}_C$ as the sum of $\boldsymbol{\alpha}_m$ and $\boldsymbol{\gamma}_D$:

$$\begin{aligned}\boldsymbol{\alpha}_C = \boldsymbol{\alpha}_m &-\frac{1}{V_D}\int_\Omega T_C\boldsymbol{G}_3'T_C^{-1}dV\bar{\boldsymbol{e}}\\ &+\frac{1}{V_D}\int_\Omega T_C\boldsymbol{G}_4'\boldsymbol{\alpha}^{*'}dV\end{aligned} \tag{10}$$

where

$$\begin{aligned}\boldsymbol{G}_3' &= \{(\boldsymbol{C}_f'-\boldsymbol{C}_m')(\boldsymbol{S}'-\boldsymbol{I}')+\boldsymbol{C}_f'\}^{-1}(\boldsymbol{C}_f'-\boldsymbol{C}_m')\\ \boldsymbol{G}_4' &= \{(\boldsymbol{C}_f'-\boldsymbol{C}_m')(\boldsymbol{S}'-\boldsymbol{I}')+\boldsymbol{C}_f'\}^{-1}\boldsymbol{C}_f'\end{aligned} \tag{11}$$

Let the density function, volume of the single fiber, and fiber volume fraction be denoted by $\rho(\theta)$, v_f, and f, respectively. Then eqs. 7 and 10 are written as follows with the use of the relation $dV = v_f\rho(\theta)d\theta$ for two-dimensional distribution of fiber orientation on x_2x_3-plane and the fact $\boldsymbol{G}_i'\boldsymbol{\alpha}^{*'}$ is not the function of θ but constant,

$$\begin{aligned}&\{\boldsymbol{I}-f\int_0^\beta T_C\boldsymbol{G}_1'T_C^{-1}\rho(\theta)d\theta(\int_0^\beta\rho(\theta)d\theta)^{-1}\}\bar{\boldsymbol{e}}\\ &= -f\int_0^\beta T_C\rho(\theta)d\theta\boldsymbol{G}_2'\boldsymbol{\alpha}^{*'}(\int_0^\beta\rho(\theta)d\theta)^{-1}\end{aligned} \tag{7'}$$

$$\begin{aligned}\boldsymbol{\alpha}_C = \boldsymbol{\alpha}_m &-f\int_0^\beta T_C\boldsymbol{G}_3'T_C^{-1}\rho(\theta)d\theta(\int_0^\beta\rho(\theta)d\theta)^{-1}\bar{\boldsymbol{e}}\\ &+f\int_0^\beta T_C\rho(\theta)d\theta\boldsymbol{G}_4'\boldsymbol{\alpha}^{*'}(\int_0^\beta\rho(\theta)d\theta)^{-1}\end{aligned} \tag{10'}$$

Here it is assumed that fibers are distributed within $0\leqq\theta\leqq\beta$ as shown in Fig. 2-a. Eq. 7(7′) represents, in general, six linear algebraic equations with six unknow components of $\bar{\boldsymbol{e}}$ and provides a solution of $\bar{\boldsymbol{e}}$, which is substituted into eq. 10(10′) to obtain $\boldsymbol{\alpha}_C$. It is shown after some calculation that $\bar{\boldsymbol{e}}$ has only three unknown components, i. e., $\bar{e}_{11}$, $\bar{e}_{22}$,and $\bar{e}_{33}$, with zero shear components.

With the use of $\boldsymbol{\alpha}^* = \boldsymbol{\alpha}_f-\boldsymbol{\alpha}_m$, we can formally obtain the following equa-

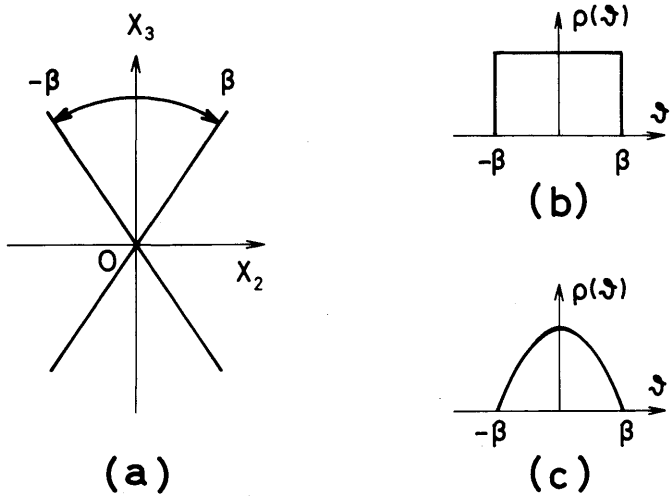

Fig. 2 Fiber orientation limit β and the type of distribution.

tions : from eq. (7′)

$$\bar{e} = A(\alpha_f - \alpha_m) \tag{12}$$

and inserting eq. (12) into eq. (10′) finally yields

$$\alpha_C = \alpha_m + B(\alpha_f - \alpha_m) \tag{13}$$

where A and B are 6×6 matrices. As our target material is isotropic, that is, $\alpha_f = \alpha_f(1,1,1)^t$ and $\alpha_m = \alpha_m(1,1,1)^t$, the normal components of α_c, $(\alpha_{c1},\alpha_{c2},\alpha_{c3})^t$, are obtained as follows,

$$\frac{\begin{bmatrix} \alpha_{c1}-\alpha_m \\ \alpha_{c2}-\alpha_m \\ \alpha_{c3}-\alpha_m \end{bmatrix}}{\alpha_f-\alpha_m} = B\begin{bmatrix} 1 \\ 1 \\ 1 \end{bmatrix} = \sum_{j=1}^{3} B_{ij} \tag{14}$$

where B_{ij} is the (i,j) component of the matrix B. B or $\sum_{j=1}^{3} B_{ij}$ has no relation to the thermal expansion coefficients of both matrix and fiber, and it will be plotted as the non-dimensional results of the present analysis, $(\alpha_c-\alpha_m)/(\alpha_f-\alpha_m)$.

3. Numerical results

The comparison with previous works was carried out in Reference 10 by the present author.

In Figs. 3-6 we will present the thermal expansion coefficients α_c of Glass/Epoxy composites as a function of distribution limit β. Material constants are given by Table 1. The effects of the type of distribution in fiber orientation on α_c are shown in Fig. 3, where fiber aspect ratio $\ell/d = 100$, and fiber volume fraction $f = 0.4$. Here α_{ci} is the normal component of α_c along the x_i direction.

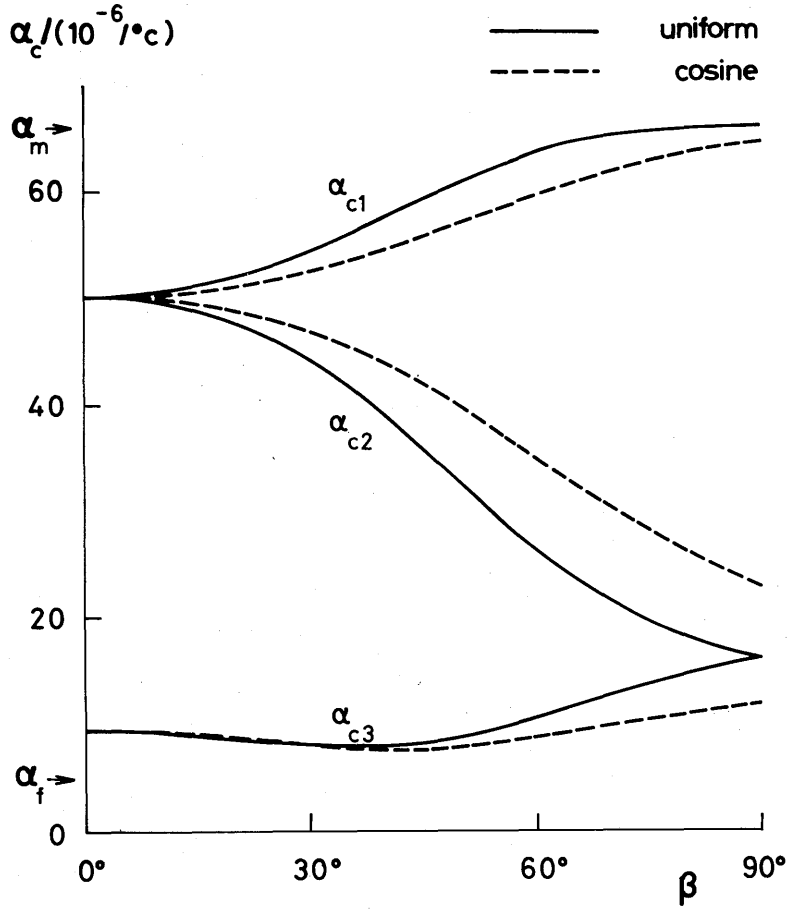

Fig. 3 Effects of distribution-type on thermal expansion coefficients of Glass/Epoxy composites α_c with distribution limit β for $\ell/d = 100$ and $f = 0.4$.

Table 1 Material Constants of Glass-Fiber and Epoxy[1)]

Young's Modulus Ratio	E_f/E_m	76/3.5(≒20)
Poisson's Ratio of Fiber	ν_f	0.2
Poisson's Ratio of Matrix	ν_m	0.38
Thermal Expansion Coefficient of Fiber	α_f	4.9*
Thermal Expansion Coefficient of Matrix	α_m	66.0*

*:($\times 10^{-6}$/°C)

The solid and dashed curves correspond to the uniform-type of distribution ($\rho(\theta)$ = constant in Fig. 2-b) and the cosine-type ($\rho(\theta) = \cos(\theta/\beta)$ in Fig. 2-c), respectively. The value of α_c for the cosine-type is obtained roughly by shifting α_c for the uniform-type to the right side as expected. Then α_{c2} is higher for the cosine-type than the uniform-type. And α_{c3} of the cosin-type is higher at small values of β and lower at large values of β due to the fact that there is the minimum for α_{c3}.

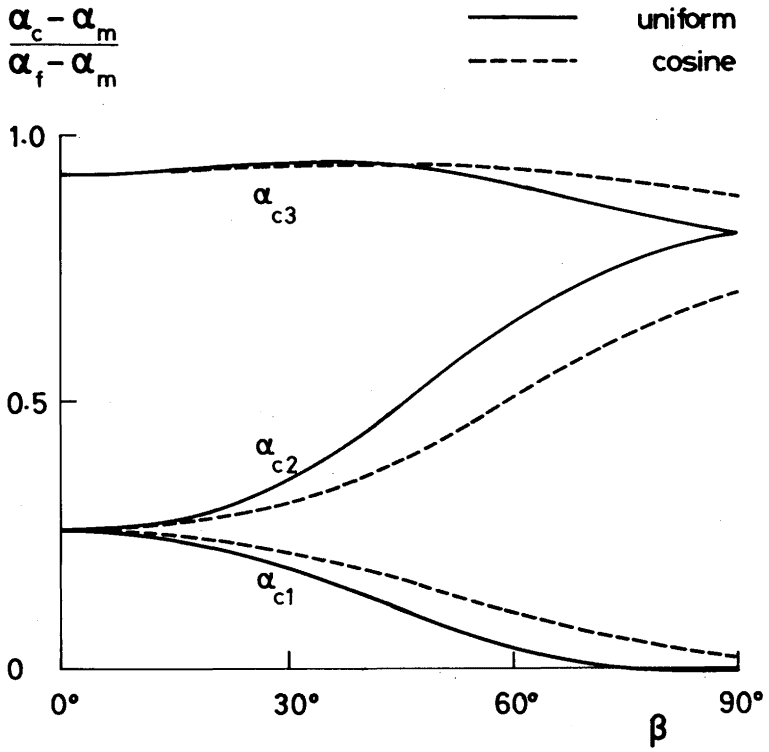

Fig. 4. Effects of distribution-type on non-dimensional value $(\alpha_c - \alpha_m)/(\alpha_f - \alpha_m)$ with β for $\ell/d = 100$ and $f = 0.4$.

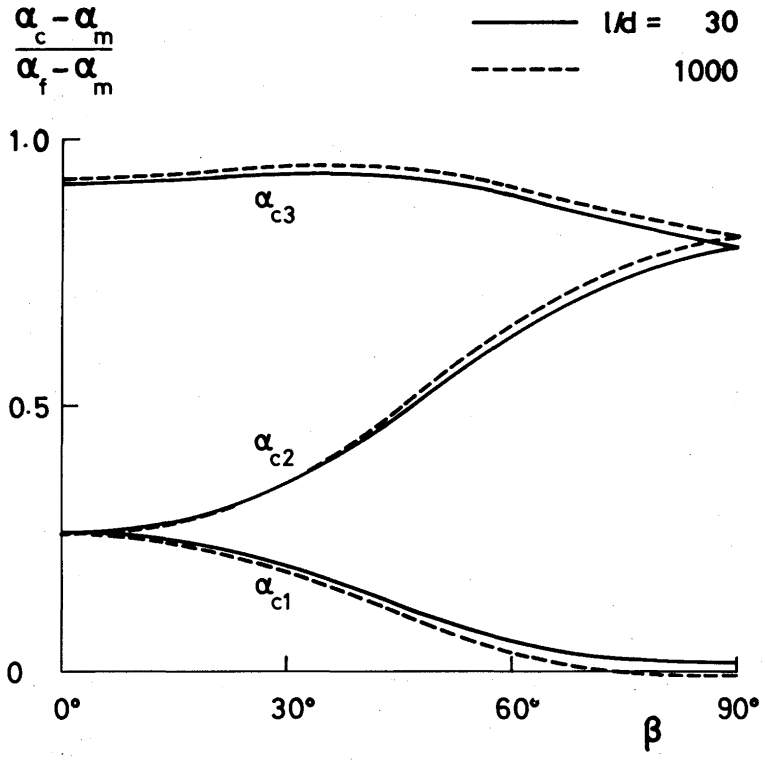

Fig. 5 Effects of fiber aspect ratio ℓ/d on $(\alpha_c-\alpha_m)/(\alpha_f-\alpha_m)$with β for uniform-type distribution and $f = 0.4$.

This phenomena was more significant in the case of the Carbon/Epoxy composite system[10),11)]. The non-dimensional representation of Fig. 3, $(\alpha_c-\alpha_m)/(\alpha_f-\alpha_m)$ in eq.(14), is given in Fig. 4. In this figure the upper curves correspond to α_{c3} and the lower one to α_{c1}, which is directly opposite to Fig. 3. The non-dimensional value is negative for $\alpha_{ci} > \alpha_m$ and larger than 1.0 for $\alpha_{ci} < \alpha_f$. The effects of fiber aspect ratio ℓ/d on $(\alpha_c-\alpha_m)/(\alpha_f-\alpha_m)$ are shown in Fig. 5 for $f = 0.4$. The solid and dashed curves are for $\ell/d = 30$ and 1000, respectively. The fiber with $\ell/d = 1000$ corresponds to the infinitely long one in this calculation. In this and following figures we consider the uniform-type of distribution. The value of α_{c3} for $\ell/d = 1000$ is smaller than the one for $\ell/d = 30$ due to the efficient reinforcement of the long fiber. To compensate the above phenomena α_{c1} for $\ell/d = 1000$ is larger than the one for $\ell/d = 30$. Then, α_{c2} for $\ell/d = 1000$ is smaller than the one for $\ell/d = 30$ at large value of β and larger at small value of β. The effects

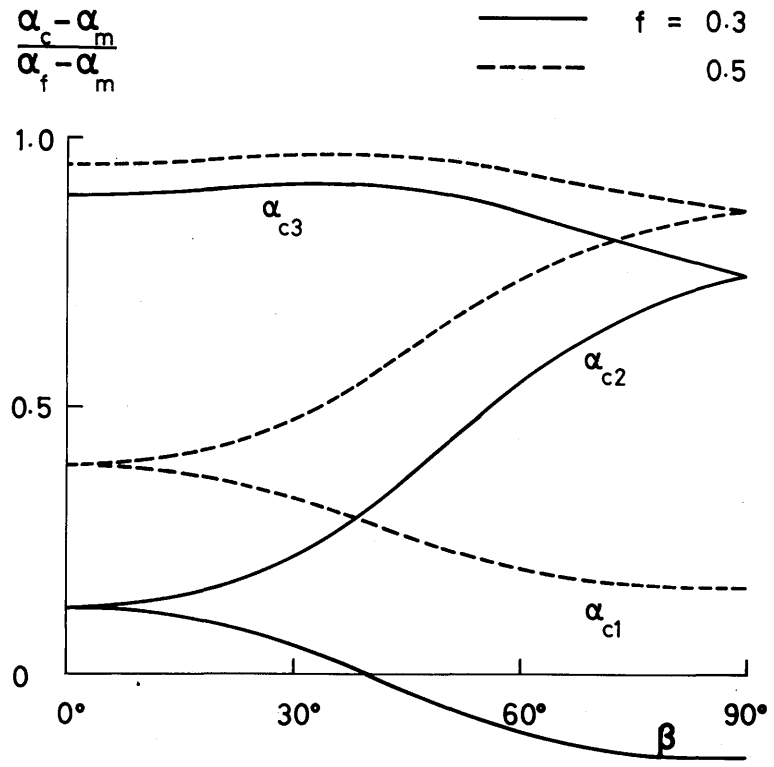

Fig. 6 Effects of fiber volume fraction f on $(\alpha_c-\alpha_m)/(\alpha_f-\alpha_m)$with β for uniform-type distribution and $\ell/d = 100$.

of fiber volume fraction f on $(\alpha_c-\alpha_m)/(\alpha_f-\alpha_m)$ are shown in Fig. 6. The value of α_c for higher volume fraction of $f = 0.5$ (dashed curve) is smaller than the one for $f = 0.3$ (solid curve) in each component. The values for $f = 0.4$ are plotted in Fig. 4 by solid curves.

We have computed the values of α_c by changing the material parameters of the matrix and fiber within the practical range to assess the degree of the effects of them and it is shown in Figs. 7-9 as a function of β. In this calculation $\ell/d = 100$, $f = 0.4$, and the data given by Table 1 are used if not mentioned otherwise. The effects of Young's modulus ratio E_f/E_m on $(\alpha_c-\alpha_m)/(\alpha_f-\alpha_m)$ are shown in Fig. 7 with $E_f/E_m = 10$(solid) and 50 (dashed curves). The results for $E_f/E_m = 20$ are plotted in Fig. 4 by solid curves. The larger value of E_f/E_m yields the smaller value of α_{c3} and larger value of α_{c1}, which is same to the case of fiber aspect ratio in Fig. 5. The value of α_{c3} is smaller than α_f at $\beta = 30°\sim50°$ for E_f

$/E_m = 50$. Practically we can not find the minimum in α_{c3} at around $\beta = 40°$ for $E_f/E_m = 10$. In Fig. 8 are shown the effects of Poisson's ratio of matrix ν_m on $(\alpha_c - \alpha_m)/(\alpha_f - \alpha_m)$. The solid and dashed curves correspond to $\nu_m = 0.3$ and 0.45, respectively. The results for $\nu_m = 0.38$ are plotted in Fig. 4 by solid curves. The matrix with larger Poisson's ratio shows larger value of α_c's especially in the case of α_{c1}. It follows from Fig. 9 that the effect of Poisson's ratio of fiber is small within the calculated range. The larger value of ν_f, 0.3 by dashed lines, yields the smaller α_c's, which is same to the case of fiber volume fraction in Fig. 6. The values for $\nu_f = 0.1$ are plotted by solid curves and those for $\nu_f = 0.2$ are shown in Fig. 4.

We can divide the effects of parameters into two groups : those are same for all components as in the cases of fiber volume fraction f, Poisson's ratio of matrix ν_m, and Poisson's ratio of fiber ν_f, and those are different in components as in the cases of fiber aspect ratio ℓ/d and Young's modulus ratio E_f/E_m. In the latter case, α_{c1} has higher values to compensate lower values of α_{c3}.

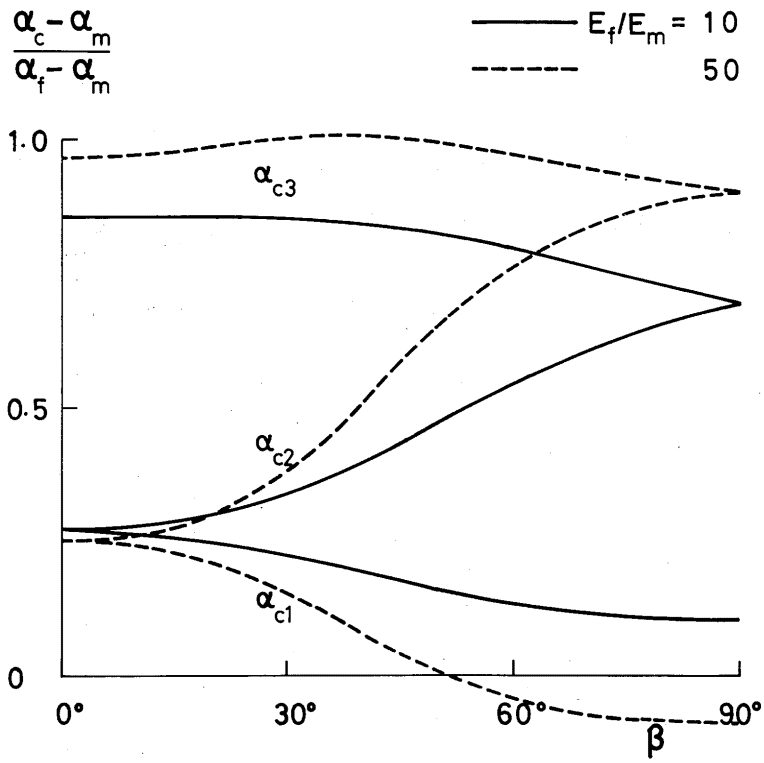

Fig. 7 Effects of Young's modulus ratio E_f/E_m on $(\alpha_c - \alpha_m)/(\alpha_f - \alpha_m)$ with β for uniform-type distribution, $\ell/d = 100$, and $f = 0.4$.

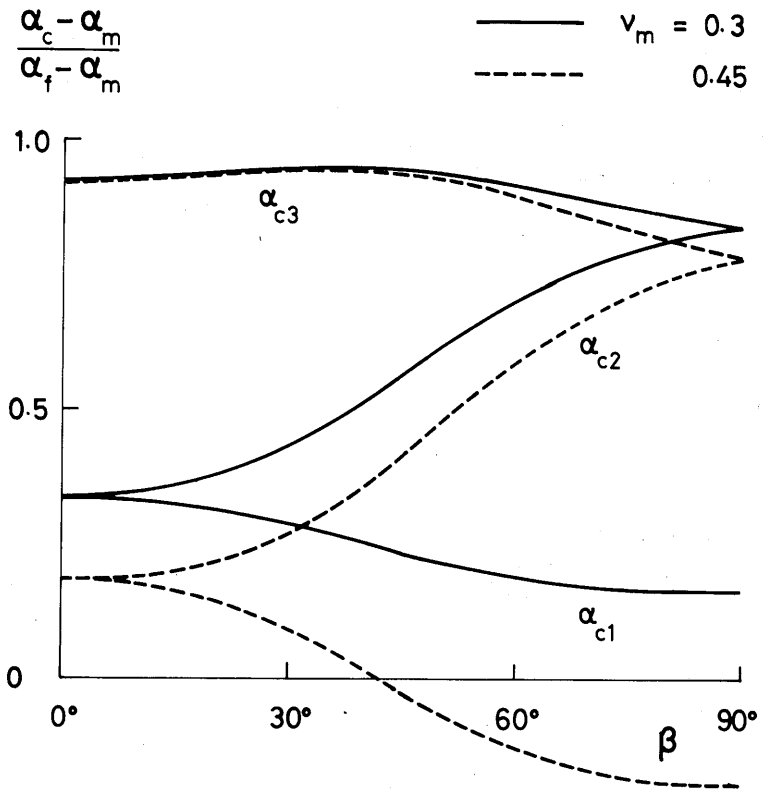

Fig. 8 Effects of Poisson's ratio of matrix ν_m on $(\alpha_c - \alpha_m)/(\alpha_f - \alpha_m)$ with β for uniform-type distribution, $\ell/d = 100$, and $f = 0.4$.

4. Conclusion

(1) The effects of the distribution limit of fiber on thermal expansion coefficients are obtained for the two-dimensional distribution of fiber orientation with both uniform-type and cosine-type fiber density functions, using the theory which is based on the Eshelby's equivalent inclusion method and average induced strain approach and takes into account the interaction among all fibers.

(2) Glass/Epoxy composites with misoriented short fibers are studied and it is pointed out that the effects of each parameter are devided into two groups : (a) higher values of both fiber volume fraction and Poisson's ratio of fiber and smaller values of Poisson's ratio of matrix yield smaller thermal expansion coefficients for all components and (b) larger values of fiber aspect ratio and Young's modulus ratio yield smaller α_{c3} and larger α_{c1}, which is true for any distribution limit β.

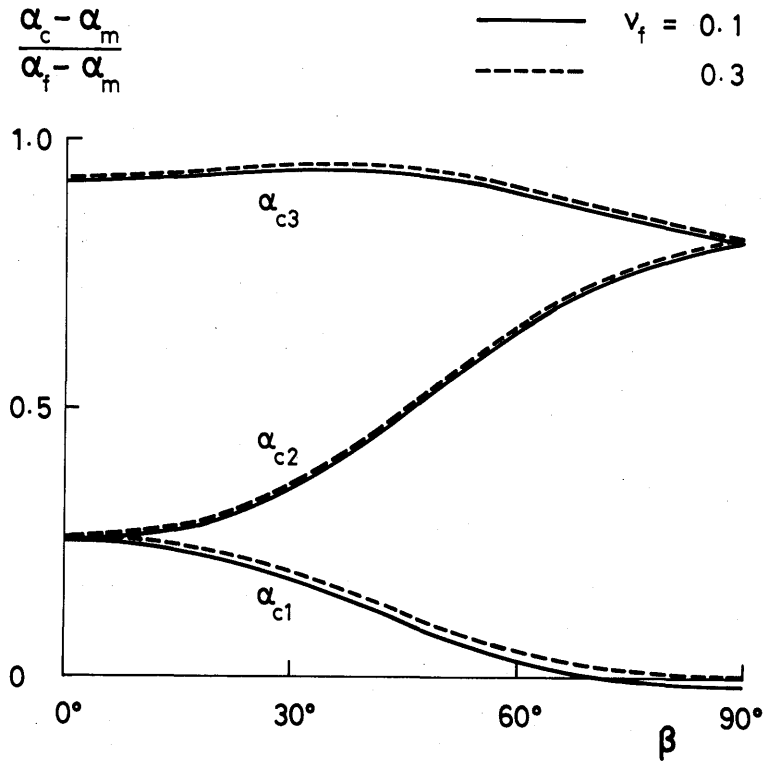

Fig. 9 Effects of Poisson's ratio of fiber ν_f on $(\alpha_c - \alpha_m)/(\alpha_f - \alpha_m)$ with β for uniform-type distribution, $\ell/d = 100$, and $f = 0.4$.

Acknowledgment

The author would like to thank Professor M. Taya of University of Delaware and Professor T. Suhara of Kyushu University for their helpful discussions and Ms. K. Hara for her skillful typing.

References

1) Hull, D., "*An Introduction to Composite Materials*," Cambridge University Press, 1981.
2) Takao, Y., Chou, T. W., and Taya, M., "Effective Longitudinal Young's modulus of Misoriented Short Fiber Composites," Journal of Applied Mechanics, Vol. 49, 1982, pp. 536-540.

3) Takao, Y., Taya, M., and Chou, T. W., "Effective Longitudinal Young's Modulus of Two-Dimensionally Misoriented Short Fiber Composites," Proceedings of ICCM-IV, 1982, Tokyo, Hayashi, T., Kawata, K., and Umekawa,S. (eds.), Japan Society for Composite Materials, 1982, pp. 1091-1098.
4) Chou, T. W. and Nomura, S., "Fiber Orientation Effects on the Thermoelastic Properties of Short-Fiber Composites," Fiber Science and Technology, Vol. 14, 1980-1981, pp. 279-291.
5) Craft, W. J. and Christensen, R. M., "Coefficient of Thermal Expansion for Composites With Randomly Oriented Fibers," Journal of Composite Materials, Vol. 15, 1981, pp. 2-20.
6) Takahashi, K., Harakawa, K., and Sasaki, T., "Analysis of Thermal Expansion Coefficients of Particle-Filled Polymers," Journal of Composite Materials (Supplement), Vol. 14, 1980, pp. 144-159.
7) Wakashima, K., Otsuka, M., and Umekawa, S., "Thermal Expansions of Heterogeneous Solids Containing Aligned Ellipsoidal Inclusions," Journal of Composite Materials,Vol. 8, 1974, pp. 391-404.
8) Eshelby, J. D., "The Determination of the Elastic Field of an Ellipsoidal Inclusion, and Related Problems," Proceedings of the Royal Society of London, Series A, Vol. 241, 1957, pp. 376-396.
9) Mura, T., "*Micromechanics of Defects in Solids*," Martinus Nijhoff Publishers, 1982.
10) Takao, Y., "Thermal Expansion Coefficients of Misoriented Short-Fiber Reinforced Composites," submitted for publication.
11) Rogers, K. F. et al., "The Thermal Expansion of Carbon Fiber-Reinforced Plastics : Part 1 The Influence of Fiber Type and Orientation," Journal of Materials Science, Vol. 12, 1977, pp. 718-734.

(Received June 30, 1983)